OncoTargets and Therapy

Dovepress
open access to scientific and medical research

Open Access Full Text Article

ORIGINAL RESEARCH

miR-19 promotes the proliferation of clear cell renal cell carcinoma by targeting the FRK–PTEN axis

This article was published in the following Dove Medical Press journal:
OncoTargets and Therapy

Zhi-Fei Jing[1,2]
Jian-Bin Bi[1,2]
Ze-Liang Li[1,2]
Xian-Kui Liu[1,2]
Jun Li[1,2]
Yu-Yan Zhu[1,2]
Xiao-Tong Zhang[1,2]
Zhe Zhang[1,2]
Zhen-Hua Li[1,2]
Chui-Ze Kong[1,2]

[1]Department of Urology, First Hospital of China Medical University, Shenyang, Liaoning 110001, People's Republic of China; [2]Institute of Urology, China Medical University, Shenyang 110001, People's Republic of China

Background: The non-receptor tyrosine kinase Fyn-related kinase (FRK) has been reported to affect cell proliferation in several cancer types. However, its effect on the proliferation of clear cell renal cell carcinoma (ccRCC) remains largely unknown.

Purpose: The objective of this study was to investigate the expression pattern and function of FRK in ccRCC. We further determined how FRK interacted with other molecules to regulate ccRCC proliferation.

Patients and methods: The expression of FRK in ccRCC samples and paired normal renal tissues from 30 patients were analyzed by immunoblotting, immunohistochemistry and quantitative PCR. Then the role of FRK in ccRCC proliferation was analyzed by Cell Counting Kit-8, colony formation assay and EdU incorporation assay. In addition, the miRNA targeting FRK was predicted through a bioinformatic approach and validated by quantitative PCR, immunoblotting and luciferase reporter assay. Finally, the underlying mechanism of FRK regulation of ccRCC proliferation was also determined.

Results: Low expression of FRK was detected in ccRCC samples and predicted poor survival for ccRCC patients. FRK inhibited the proliferation of ccRCC cells via phosphorylating downstream PTEN. miR-19 was identified as a novel suppressor of FRK in renal cancer cells and it promoted the proliferation of ccRCC by inhibiting the FRK–PTEN axis.

Conclusion: Our results unravel a new regulatory mechanism involved in ccRCC proliferation and may be useful in the identification of therapeutic targets for ccRCC.

Keywords: clear cell renal cell carcinoma, miR-19, miR-17~92 cluster, FRK, PTEN, proliferation, oncomiR-1

Introduction

Renal cell carcinoma (RCC) is the second most common cancer in the urological system and accounts for ~3% of malignant neoplasms worldwide.[1] More than 90% of kidney tumors are renal cell carcinomas (RCCs), which arise from the epithelial lining of the proximal convoluted tubule.[2] Clear cell renal cell carcinoma (ccRCC) is the most common (70%–80%) and most aggressive histological subtype of RCC.[3] Surgery remains the mainstay of treatment for patients with localized ccRCC. However, ~25%–30% of metastatic lesions are detected at initial diagnosis and are resistant to chemotherapy and radiotherapy.[4] Although great advances have been made in the therapeutic strategies in the past decade, treatment options for metastatic ccRCC are still limited. Uncontrolled cellular proliferation is a hallmark of all malignancies; hence, identifying novel proliferation-associated molecules will increase our understanding of ccRCC and improve treatment and prognosis for ccRCC patients.

Correspondence: Chui-Ze Kong; Zhen-Hua Li
Department of Urology, First Hospital of China Medical University, 155 North Nanjing Street, Heping, Shenyang, Liaoning 110001, China
Tel +86 24 8328 3722; +86 24 8328 2711
Email kongchuize_cmu@sina.cn; lizhenhua024@sina.com

submit your manuscript | www.dovepress.com
Dovepress
http://dx.doi.org/10.2147/OTT.S199238

miRNAs are small noncoding RNAs (19–22 nt), known to negatively regulate their target genes through direct binding with the 3′-untranslated regions (UTRs) of target mRNAs.[5,6] Increasing studies revealed that miRNAs were implicated in the development and progression of RCC.[7–9] miR-19a and miR-19b, two key oncogenic components of the miR-17~92 cluster, belong to the same miRNA family (miR-19). They differ in only one nucleotide outside of the seed sequence and are therefore likely to target the same mRNAs.[10] Although miR-19 plays an oncogenic role in multiple malignancies,[11–13] its role in ccRCC remains largely unknown. To date, only a few target genes have been validated.[14,15] Additional studies are necessary to identify more target genes of miR-19 and thereby elucidate the functions of miR-19 in ccRCC.

FRK, also known as protein tyrosine kinase 5, was originally discovered in breast cancer cells.[16] FRK was initially characterized as a tumor suppressor that arrested cell growth and suppressed tumorigenesis;[17–20] however, recent studies indicated that FRK contributed to the progression of several malignancies as well.[21,22] These contradictory results suggest that the function of FRK is cell- and tissue-type specific. Thus far, the expression and function of FRK in ccRCC remain unclear, and how FRK is regulated in ccRCC requires further investigation.

Here, we investigated the expression of FRK in ccRCC and determined its impact on cell proliferation. We further identified and validated miR-19 as a novel regulator of FRK and revealed how miR-19 interacted with the FRK–PTEN axis to modulate renal cancer cell proliferation.

Materials and methods

Cell culture and transfection

Human cell lines 293T, HK-2, CAKI-1, ACHN, A498, 769P, 786-O, and OS-RC-2 were obtained from the Cell Bank of Shanghai Institute of Cell Biology (Chinese Academy of Medical Science, Shanghai, China). 769-P, 786-O, and OS-RC-2 were cultured in RPMI-1640 (HyClone, Logan, UT, USA) supplemented with 10% FBS (HyClone) at 37°C with 5% CO_2. ACHN and A498 cells were cultured in MEM (HyClone) with 10% FBS. CAKI-1 cells were cultured in McCoy's 5a medium (HyClone) modified with 10% FBS. HK-2 cells were cultured in DMEM/F12 (HyClone) medium with 10% FBS. 293T cells were cultured in DMEM (HyClone) with 10% FBS. Transfection was performed using Lipofectamine 3000 Transfection Reagent (Thermo Fisher Scientific, Waltham, MA, USA) according to the manufacturer's instructions.

Tissue specimens

Thirty renal tumor specimens and paired normal renal tissues were collected from patients undergoing radical or partial nephrectomy (laparoscopic or open) in the Urology Department, First Hospital of China Medical University (Shenyang, China) for a renal mass between July 2016 and November 2017. The Ethics Committee of China Medical University approved this study according to the Declaration of Helsinki. Written informed consent was obtained from all individual participants included in the study.

Antibodies and reagents

Antibodies used in this study were obtained as follows: anti-FRK (abs133481; Absin, Shanghai, China), anti-PTEN (ab32199; Abcam, Cambridge, MA, USA), anti-GAPDH (5174; Cell Signaling, Danvers, MA, USA).

Western blot analysis

Cells were rinsed with cold PBS and homogenized with RIPA lysis buffer supplemented with 1 nM PMSF (Beyotime, Shanghai, China) and phosphatase inhibitor cocktail (MedChem Express, Shanghai, China). Afterward, 30 μg of whole cell lysates was separated by 4%–20% SDS-PAGE and electrophoretically transferred onto a polyvinylidene fluoride membrane (EMD Millipore, Billerica, MA, USA). The membrane was washed with TBST, blocked with 5% nonfat milk diluted in TBST for 1 hour and then incubated with appropriate primary antibodies overnight at 4°C. The membrane was washed and then incubated with HRP-conjugated secondary antibodies for 1 hour at 37°C. Bands were visualized with enhanced chemiluminescence reagents (Transgen Biotechnology, Beijing, China) and scanned using a DNR Microchemi imaging system (DNR Bio-Imaging System, Ltd., Jerusalem, Israel). Protein quantification was conducted using ImageJ software.

RNA extraction and real-time quantitative PCR (qPCR)

Total RNA was extracted using the Eastep Super Total RNA Extraction Kit (Promega Corporation, Fitchburg, WI, USA). miRNA was extracted using the miRcute miRNA Isolation Kit (TIANGEN Biotech, Beijing, China). Total RNA concentrations were determined by measuring the optical density at a wavelength of 260 nm. Then, the first-strand cDNA was synthesized using a reaction mixture containing 500 ng of total RNA, 2 μL 5× PrimeScript RT Master Mix (TaKaRa, Dalian, China), and RNase-free water at a total volume of

10 μL. For microRNAs, cDNA was synthesized using the Mir-XTM miRNA First-Strand Synthesis Kit (TaKaRa). qPCR was conducted using SYBR Green PCR Master Mix (TaKaRa) on a LightCycler 480 Real-Time PCR instrument (Hoffman-La Roche Ltd., Basel, Switzerland). The final 25 μL of the reaction mixture contained 12.5 μL TB Green Premix Ex TaqII (2×), 0.4 μM of each primer, and 2 μL cDNA templates. To confirm the specificity of the amplified product, a melting curve analysis was performed. The primers used for target genes were purchased from Sangon Biotech (Shanghai, China). The sequences of primers were as follows (in the 5′–3′ orientation):

FRK forward, 5′-CTCTGGGAGTACCTAGAACCC-3′;

FRK reverse, 5′-AGCCTGGTAATCAAACAAAGCC-3′;

GAPDH forward, 5′-TGTGGGCATCAATGGATTTGG-3′;

GAPDH reverse, 5′-ACACCATGTATTCCGGGTCAAT-3′;

hsa-miR-19a-3p forward, 5′-ACACTCCAGCTGGGAGTCAAAACGTATCTAA-3′;

and hsa-miR-19b-3p forward, 5′-ACACTCCAGCTGGGAGTCAAAACGTACCTAA-3′;

snRNA U6 and GAPDH were used as internal controls for miRNA and mRNA, respectively. Data are presented as relative quantification based on the calculation of $2^{-\Delta\Delta Ct}$.

Immunohistochemistry

Specimens that were previously formalin-fixed and paraffin-embedded were sliced into 4-μM sections and processed for deparaffinization and then rehydration. Antigen retrieval, suppression of endogenous peroxidase activity, and 10% BSA blocking were performed before primary antibody incubation. FRK antibodies were used as primary antibodies for overnight incubation at 4°C. The slides were subsequently incubated with peroxidase-conjugated secondary antibody (ZSGB Bio, Beijing, China) for 90 min, and a solution of the peroxidase-labeled polymer, 2,4-diaminobutyric acid, was used for signal development for 1 minute. The sections were counterstained with hematoxylin followed by dehydrating and mounting.

Cell proliferation assays

The effects of FRK on cell proliferation were measured by CCK-8, 5-ethynyl-2′-deoxyuridine (EdU) incorporation, and colony formation assays. ACHN, CAKI-1, and 786-O cells were used in the CCK-8 assays, and 2,000 cells were seeded in 96-well plates containing 100 μL of medium per well and incubated at 37°C. Ten microliters of CCK-8 reagent (Dojindo, Tokyo, Japan) was added and coincubated for 1 hour at the indicated time points. The absorbance value at a wavelength of 450 nm, which was proportional to the total number of cells per well, was then measured with a microplate reader (Model 680; Bio-Rad laboratories, Hercules, CA, USA). The results represent the average of three independent replicates. For EdU incorporation assays, EdU (10 mM; RiboBio, Guangzhou, China) was added to the culture medium and incubated for 4 hours. The 786-O cells were then fixed and stained with Hoechst 33342. EdU-positive cells (proliferating cells) were observed and counted in five randomly selected fields under a fluorescence microscope. The ratio of the number of EdU-positive cells per field to the number of Hoechst 33343-positive cells in the same field was used to quantify the cell proliferation. For the colony formation assay, four hundred 786-O cells per well were plated on six-well plates, and 10 days after seeding, cell colonies were stained with 0.5% crystal violet solution and counted.

Phos-tag analysis

The proteins were separated on 10% SDS-polyacrylamide gels prepared with 20 μM phosbind acrylamide (APExBIO, F4002) and 40 μM $ZnCl_2$. Gels were electrophoresed at 120 V for 1 hour. Prior to transfer, the gels were first equilibrated in transfer buffer containing 5 mM EDTA for 10 minutes three times and then in transfer buffer without EDTA for 10 minutes. Protein transfer from the phos-tag acrylamide gel to the PVDF membrane was performed for 2 hours at 350 mA, and then the blot was probed with the anti-PTEN antibody.

Luciferase assay

Reporter constructs containing the 3′-UTR of FRK were cloned into the pGL3-control vector. 293T cells were transiently transfected with the 3′-UTR reporter constructs (2 μg/well in six-well plates) and 10 nmol/L of the miR-19a/b-3p mimics (GenePharma, Shanghai, China) using Lipofectamine 3000 Transfection Reagent (Thermo Fisher Scientific). The activity of the 3′-UTR reporter constructs was normalized to the Renilla luciferase activity. After incubation for 48 hours, the cells were lysed with passive lysis buffer (Promega Corporation), and their activity was assessed using a Dual-Luciferase Assay Kit (Promega Corporation) according to the manufacturer's protocol.

Statistical analysis

The results are presented as the means ± standard deviation. Where appropriate, two-sample *t*-tests and ANOVA were

used. Correlations were calculated according to Pearson correlation. All tests were performed using GraphPad Prism 7 Software (GraphPad Software, Inc., La Jolla, CA, USA), and $P<0.05$ was considered significant. All experiments were performed at least three times.

Results

Reduced FRK expression was detected in ccRCC and predicted poor survival for ccRCC patients

The expression of FRK in ccRCC and paired normal renal tissues was determined using qPCR, immunoblotting, and IHC. qPCR showed that the expression of FRK mRNA was lower in ccRCC tissues than in normal renal tissues (Figure 1A). The results from immunoblot analysis also indicated that FRK protein expression was lower in ccRCC (Figure 1B and C). For the immunohistochemistry, strong staining for FRK was detected in the cytoplasm of renal tubular epithelium, while in ccRCC tissues, only weak staining was detected in the cytoplasm of cancer cells (Figure 1D). Analysis of the TCGA KIRC data set showed that the FRK transcript level was lower in ccRCC than in normal renal tissues (Figure S1A–C).[23] In addition, the analysis based on TCGA KIRC data sets indicated that low

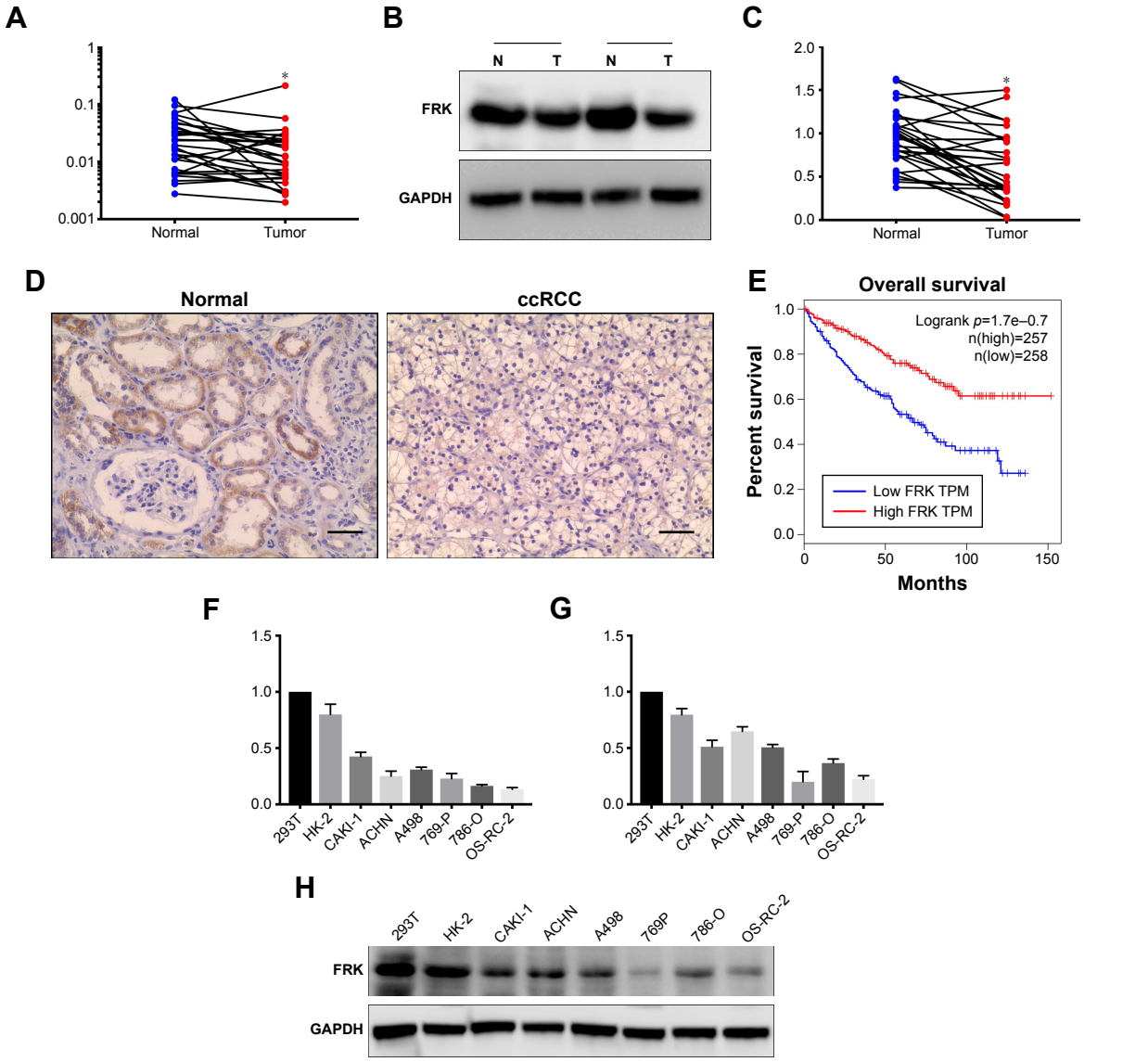

Figure 1 Expression of FRK in ccRCC tissue samples and cell lines. Quantitative PCR analysis of FRK mRNA expression in pair-matched ccRCC and normal renal tissues. (**A**) The expression of FRK mRNA was normalized to GAPDH. (**B**) Immunoblotting of FRK protein in normal (N) and paired tumor tissues (T). GAPDH was used as the loading control. (**C**) Relative FRK protein expression in ccRCC and paired normal renal tissues after normalizing to GAPDH. (**D**) Immunohistochemistry analysis of FRK expression in normal renal tissues and paired ccRCC tissues. (**E**) Kaplan–Meier curve for TCGA data sets in 515 KIRC patients. Relative expression of (**F**) FRK mRNA and (**G**) FRK protein in 293T and HK-2 cells and different renal cancer cell lines. (**H**) Immunoblotting of FRK protein in different cell lines (*$P<0.05$).
Abbreviation: ccRCC, clear cell renal cell carcinoma.

FRK expression in the ccRCC predicted poor overall survival for ccRCC patients (Figure 1E).

The endogenous expression of FRK in 293T and HK-2 kidney cells and different renal cancer cell lines was also determined by qPCR and immunoblot analyses. The results showed that the expression of FRK was lower in renal cancer cell lines than that in HK-2 kidney cells and 293T cells at both the mRNA and protein levels (Figure 1F–H).

FRK inhibited the proliferation of ccRCC via PTEN

The effect of FRK on the proliferation of renal cancer cell lines was determined using CCK-8, EdU incorporation, and colony formation assays. The CCK-8 results revealed that FRK knockdown promoted the growth of ACNH, CAIK-1, and 786-O cells, whereas FRK overexpression markedly reduced the growth of renal cancer cells compared with control cells (Figure 2A–C). In the colony formation assay, FRK knockdown in 786-O cells increased the number of 786-O cell colonies, while FRK overexpression led to a lower number of cell colonies (Figure 2D). Similar results were observed in the EdU incorporation assays in which FRK interference increased the percentage of EdU-positive 786-O cells, while FRK overexpression significantly reduced the percentage of EdU-positive cells (Figure 2E).

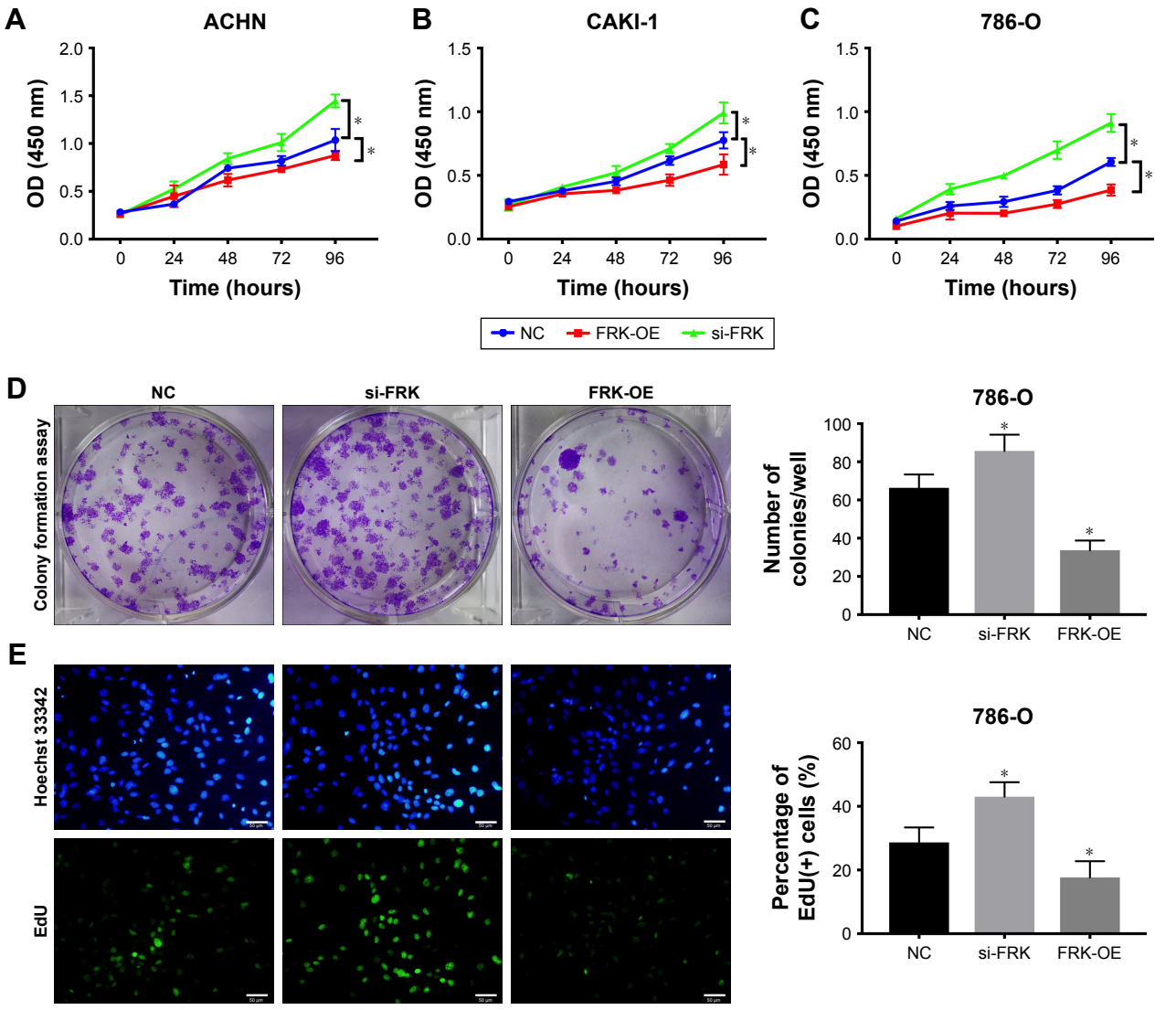

Figure 2 (**A**–**C**) Effects of FRK on the proliferation of renal cancer cells. CCK-8 analysis of the effects of FRK on the proliferation of ACHN, CAKI-1, and 786-O cells. The results are presented as the mean optical density (OD) at 450 nm for triplicate wells. (**D**) Effects of FRK knockdown or overexpression on cell colony formation in 786-O cells. Four hundred 786-O cells were seeded per well and cultured for 10 days, then the cell colonies were stained with 0.5% crystal violet and counted. (**E**) EdU incorporation assays were used to determine the effects of FRK on 786-O cell proliferation. The ratio of EdU-positive cells (green) per field to the number of Hoechst 33342-positive cells (blue) in the same field was calculated in five random fields. The results are presented as the mean ± SD of three independent experiments (*$P<0.05$).
Abbreviation: EdU, 5-ethynyl-2′-deoxyuridine.

Previously, PTEN was identified as a substrate of FRK.[19] FRK phosphorylated PTEN at Tyr336 to modulate PTEN stability and function. Here, we found that FRK protein expression also correlated with PTEN protein levels in renal cancer cells. FRK overexpression increased PTEN protein expression in ACHN and CAKI-1 cells, whereas FRK knockdown induced a reduction in PTEN protein expression (Figures 3A and S3A). In addition, FRK overexpression promoted the phosphorylation of PTEN (Figures 3B and S3B).

Since PTEN is also a critical regulator of cell proliferation and cell cycle progression,[24,25] to determine whether PTEN is involved in the growth inhibitory effect of FRK on renal cancer cells, si-PTEN was used in addition to FRK overexpression vectors in CCK-8 and EdU incorporation assays (Figures 3D and E and S3C and D). The results showed that FRK-induced growth suppression can be alleviated by PTEN interference, suggesting that PTEN plays a role in FRK-mediated growth suppression in renal cancer cells.

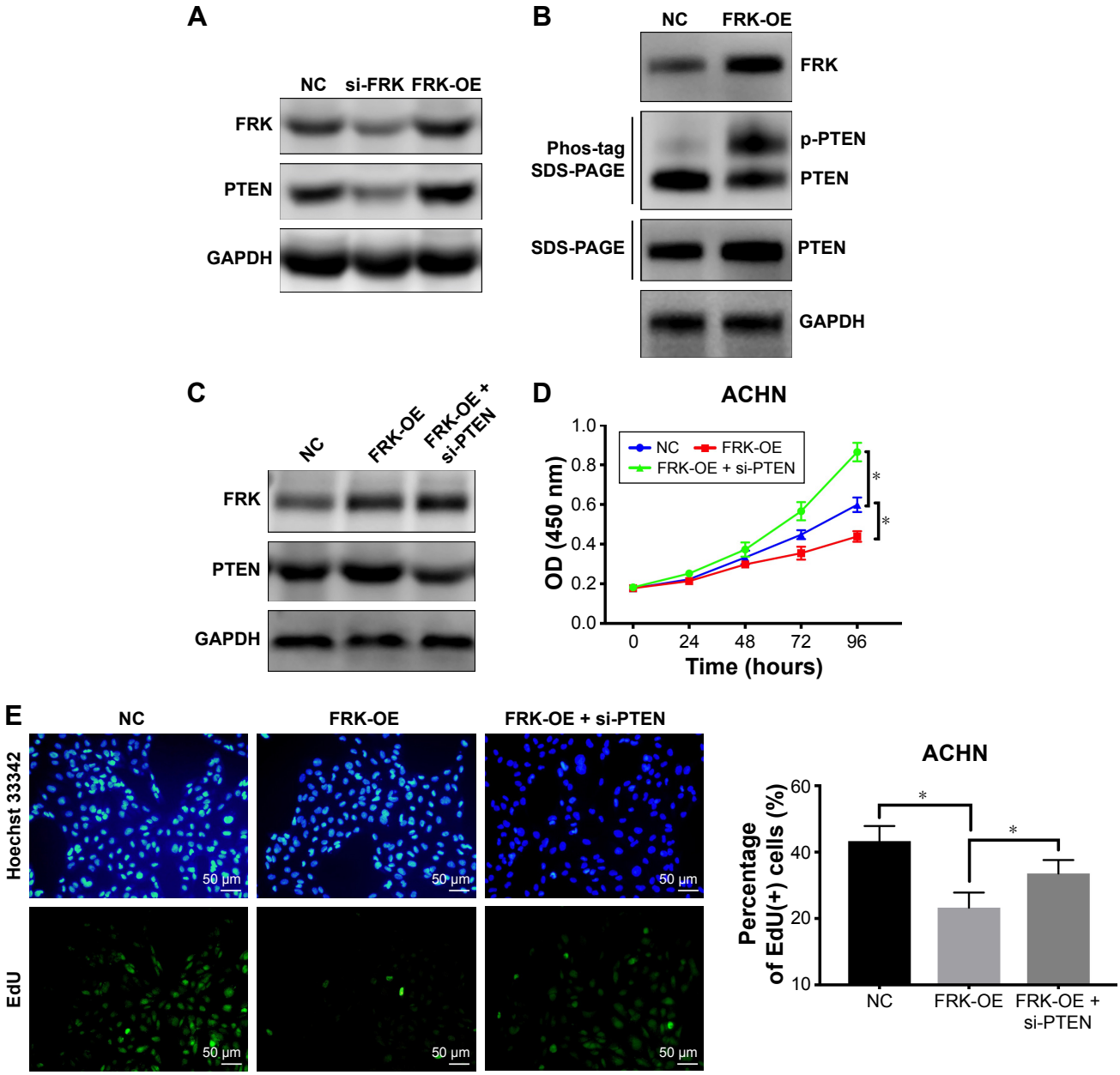

Figure 3 (**A**) The growth inhibitory effect of FRK was mediated via PTEN. Immunoblot analysis of PTEN in ACHN cells following FRK knockdown or overexpression. (**B**) The effects of FRK overexpression on the phosphorylation of PTEN in ACHN cells were analyzed by a Phos-tag assay. Immunoblots for total PTEN were also performed on normal SDS-PAGE gels. (**C**) The intervention of FRK and PTEN in ACHN cells was validated by immunoblotting. The effects of FRK overexpression with or without si-PTEN on the proliferation of ACHN cells were analyzed by (**D**) CCK-8 and (**E**) EdU incorporation assays. The results are presented as the mean ± SD of three independent experiments (*$P<0.05$).

Abbreviation: EdU, 5-ethynyl-2′-deoxyuridine.

miR-19 was identified and validated as a direct regulator of FRK

Over the past decade, an increasing number of studies have shown that miRNAs are involved in RCC development and progression. FRK downregulation could also be a result of dysregulated miRNAs in ccRCC. Thus, we searched starBase (http://starbase.sysu.edu.cn/index.php) for predicted miRNAs that potentially targeted FRK for inhibition.[26,27] Several features of the top-ranked miRNA, miR-19a/b-3p, attracted our attention. miR-19a/b-3p was not only upregulated in ccRCC but also inversely correlated with FRK expression (Figure S2A and B). In addition, data from TCGA KIRC showed that high expression of miR-19a-3p and miR-19b-3p in ccRCC predicted poor survival in ccRCC patients (Figure S2C). Furthermore, PTEN was a common downstream effector shared by both miR-19 and FRK. These findings suggested that miR-19 may play a role in ccRCC proliferation by interacting with FRK and PTEN.

To broaden our knowledge of miR-19 in ccRCC, we first examined the expression of miR-19a-3p and miR-19b-3p in ccRCC specimens. The qPCR results showed that the expression of both miR-19a-3p and miR-19b-3p was higher in ccRCC tissues than in normal renal tissues (Figure 4A and B). Furthermore, the expression of miR-19a-3p and miR-19b-3p was inversely correlated with FRK mRNA expression in ccRCC (Figure 4C and D) which was consistent with the findings from the KIRC database. Since miR-19a-3p and miR-19b-3p belong to the same miRNA cluster, it is unsurprising that they show a similar pattern in the expression and correlation with FRK.

To confirm that FRK was regulated by miR-19a/b-3p, qPCR, immunoblot, and luciferase reporter assays were also employed. The transfection of miR-19a/b-3p mimics reduced the expression of both FRK mRNA and protein in ACHN cells, while miR-19a/b-3p inhibitors increased FRK expression (Figure 4E–I). Similar results were also

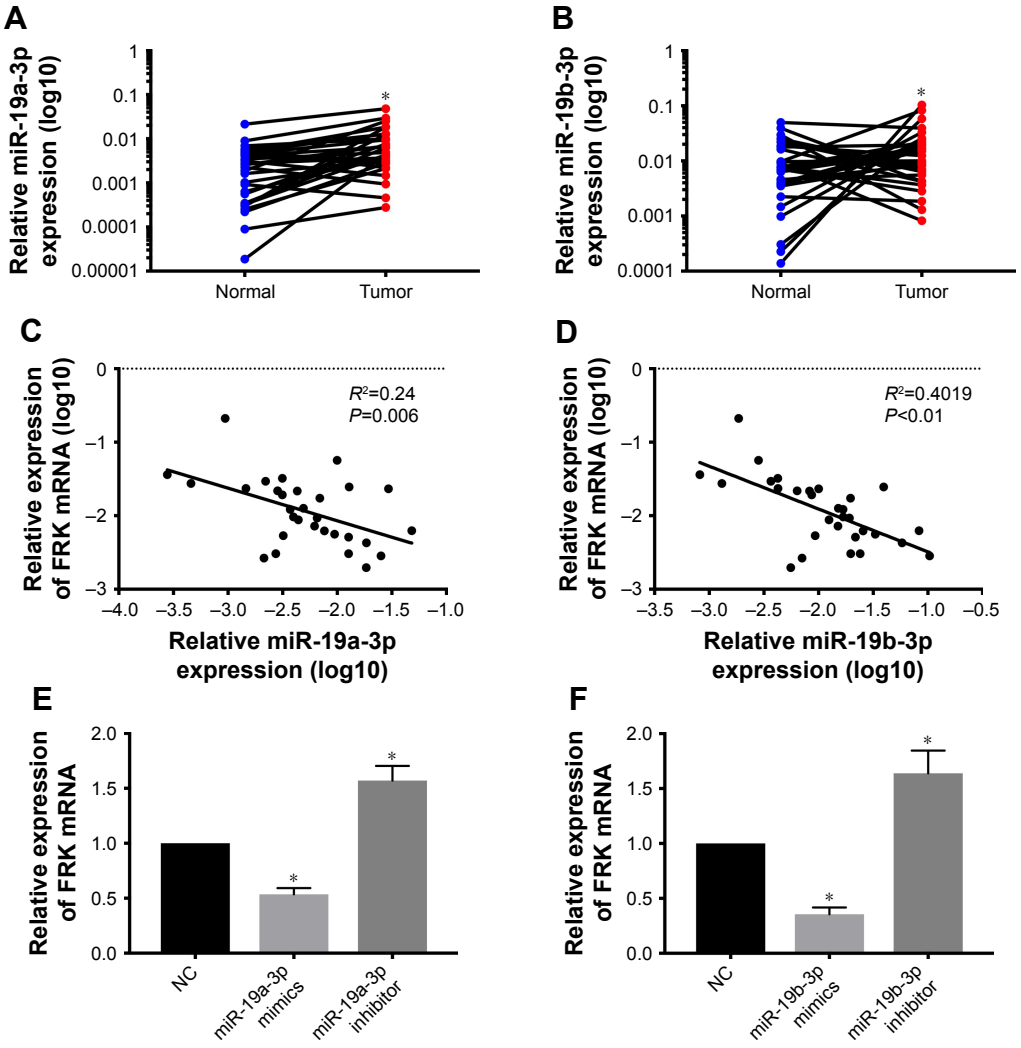

Figure 4 (*Continued*)

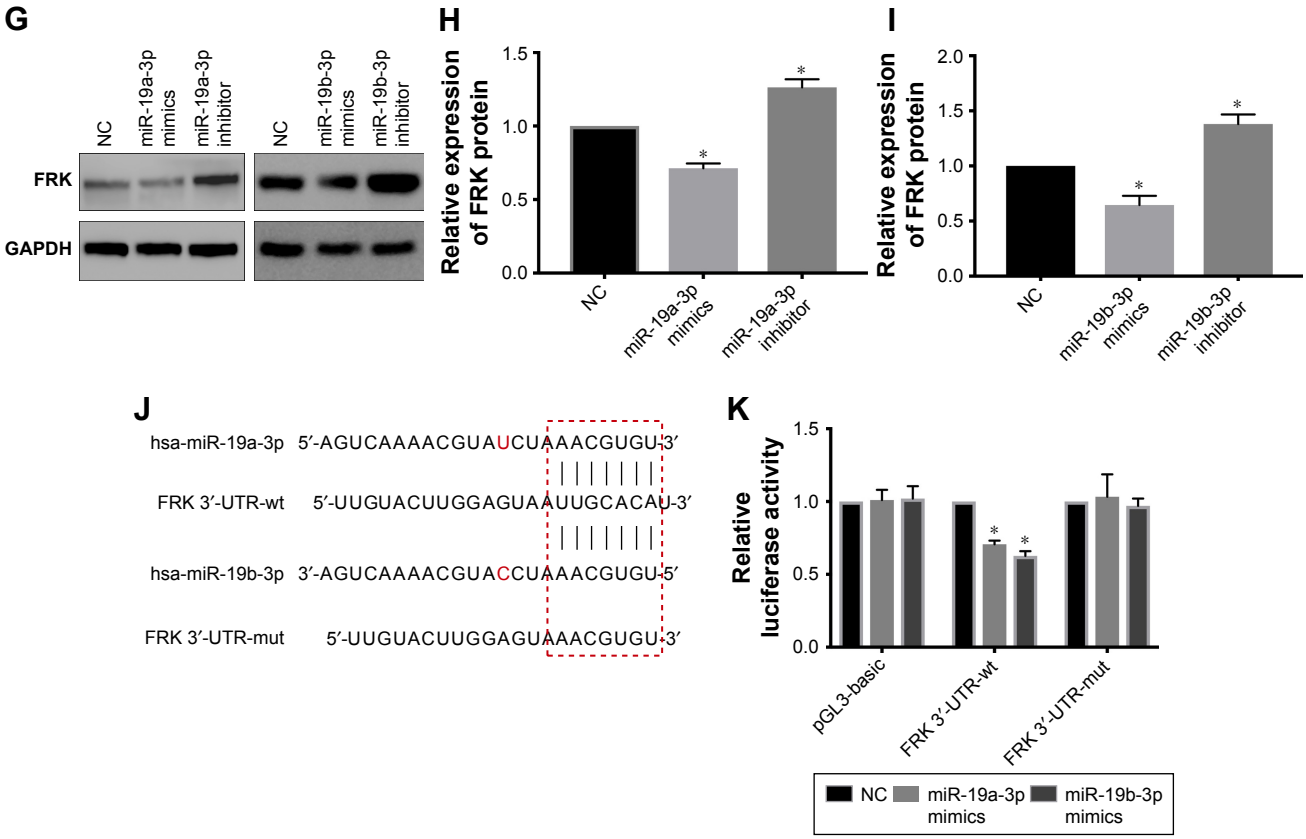

Figure 4 miR-19a/b-3p inhibited FRK expression by targeting the 3′-UTR of FRK mRNA. Quantitative PCR analysis of miR-19a-3p and miR-19b-3p expression in pair-matched ccRCC and normal renal tissues. (**A**, **B**) The expression of miR-19a-3p or miR-19b-3p was normalized to U6 expression. (**C**, **D**) Correlation of miR-19a/b-3p with FRK mRNA expression in 30 ccRCC tissue samples. (**E**, **F**) The mRNA expression of FRK in ACHN cells after transfecting with miR-19a/b-3p mimics or inhibitors is presented as bar graphs. The protein expression of FRK in ACHN cells after transfecting with miR-19a/b-3p mimics or inhibitors was analyzed by (**G**) immunoblotting and (**H**, **I**) presented as bar graphs. (**J**) Alignment of putative binding sequence in the 3′-UTR of FRK mRNA and the miR-19a/b-3p seed sequence. Red letters indicate the difference between miR-19a-3p and miR-19b-3p sequences. The red box indicates the putative binding sequence and mutation. Luciferase reporter constructs containing wild type or mutated FRK 3′-UTR were cotransfected with miR-19a/b-3p mimics or control into 293T cells. Forty-eight hours later, cells were lysed for the (**K**) luciferase assay. The results are presented as the mean ± SD of three independent experiments (*$P<0.05$).

Abbreviations: ccRCC, clear cell renal cell carcinoma; UTR, untranslated region.

observed in CAKI-1 cells (Figure S4A–C). In the luciferase reporter assay, we observed a significant downregulation of luciferase activity upon cotransfection of miR-19a/b-3p mimics and wild-type FRK 3′-UTR compared to the control group (Figure 4K). However, cotransfection of miR-19a/b-3p mimics and plasmids with a mutation in the predicted binding site did not result in a reduction of luciferase activity. These findings indicated a direct regulation of FRK by miR-19a/b-3p through binding to the 3′-UTR of the FRK mRNA.

miR-19 regulated the proliferation of ccRCC by targeting FRK–PTEN

The effect of miR-19a-3p and miR-19b-3p on the proliferation of renal cancer cells was also determined. The results from CCK-8 revealed that both miR-19a-3p and miR-19b-3p mimics enhanced the proliferation of ACHN cells in comparison with control groups, whereas miR-19a-3p and miR-19b-3p inhibitors suppressed the proliferation of ACHN cells (Figure 5A and B). In EdU incorporation assays, more EdU positively stained cells were observed in ACHN cells transfected with miR-19a/b-3p mimics compared with the control group, while transfection of miR-19a/b-3p inhibitors reduced the percentage of EdU-positive cells (Figure 5C and D).

Since miR-19a-3p and miR-19b-3p differ in only one nucleotide outside the seed sequence, it can be expected that they share the same target mRNAs and produce similar effects on cell proliferation. Hence, only a miR-19b-3p inhibitor was employed in the following experiments. To determine whether the growth inhibitory effect of miR-19 was mediated via the FRK–PTEN axis, si-FRK and si-PTEN were used in addition to miR-19b-3p inhibitors in CCK-8 and EdU assays. Although transfection of the miR-19b-3p inhibitor suppressed the growth of ACHN cells, this suppression could be partially rescued by FRK or PTEN

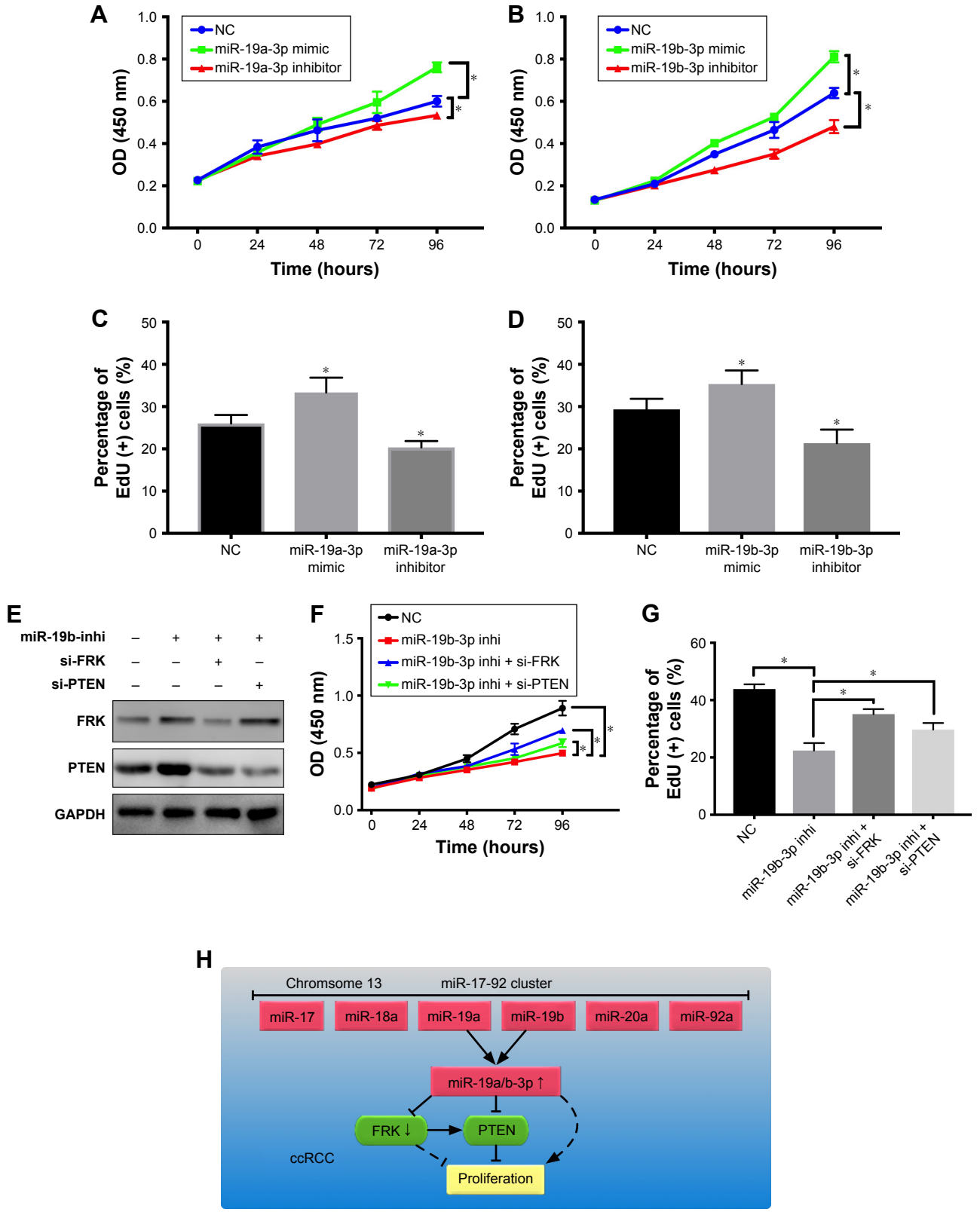

Figure 5 miR-19a/b-3p promotes renal cancer cell proliferation via the FRK–PTEN axis. (**A**, **B**) The effects of miR-19a/b-3p on the proliferation of ACHN cells were analyzed by CCK-8 assays. The results are presented as the mean optical density (OD) at 450 nm for triplicate wells. (**C**, **D**) The effects of miR-19a/b-3p on the proliferation of ACHN cells assessed by EdU assays are presented as bar graphs. (**E**) Immunoblot analysis of FRK and PTEN protein expression in ACHN cells after different treatments. The effects of the miR-19b-3p-FRK-PTEN axis on proliferation of ACHN cells were analyzed by (**F**) CCK-8 assays and (**G**) EdU assays. (**H**) Schematic diagram of the miR-19 signaling in the promotion of renal cancer cell proliferation. Dashed lines indicate indirect regulation. The results are presented as the mean ± SD of three independent experiments (*$P<0.05$).

Abbreviation: EdU, 5-ethynyl-2′-deoxyuridine.

knockdown (Figure 5E–G), suggesting the involvement of the FRK–PTEN axis in the miR-19-mediated suppression of renal cancer cell proliferation.

Discussion

This study found that FRK expression was reduced in ccRCC compared to normal renal tissues and that FRK functioned as a tumor suppressor in renal cancer cells by inhibiting cell proliferation. Furthermore, FRK was negatively regulated by miR-19a-3p and miR-19b-3p, and the expression of these miRNAs was upregulated in ccRCC. We also found that miR-19a-3p and miR-19b-3p could promote the proliferation of renal cancer cells by targeting the FRK–PTEN axis.

Earlier studies have attributed a tumor suppressive role to FRK due to its growth inhibitory effect in breast and glial cancers.[17,18] However, recent studies indicate that FRK contributes to tumor progression in several malignancies.[21,22,28] These contradictory results suggest that the function of FRK is cell- and tissue-type specific and must be determined through a case-by-case approach. To the best of our knowledge, this study is the first to provide evidence of reduced FRK expression in ccRCC and its role in suppressing cell proliferation by targeting PTEN. However, the role of FRK in apoptosis, migration, and other biological processes is still unclear and awaits further investigation. In addition, studies aimed at identifying and characterizing more substrates and binding partners of FRK will be necessary to improve our understanding of FRK.

The miR-17~92 cluster, which includes six mature miRNAs (miR-17, miR-18a, miR-19a, miR-19b, miR-20a, and miR-92a), is believed to be the first miRNA cluster with oncogenic potentials.[29] Chow et al was the first to report the upregulation of miR-19~92 in ccRCC and found the growth promoting effect of two members of this cluster (miR-17-5p and miR-20a).[30] Recent studies found that miR-19 plays an oncogenic role by targeting PIK3CA and RhoB in ccRCC.[14,15] Here, we identified FRK as a novel downstream effector of miR-19a-3p and miR-19b-3p, expanding the target gene spectrum of miR-19. Notably, PTEN was reported to be a direct target of both miR-19 and FRK in previous studies.[19,31,32] The discovery of a regulatory relationship between miR-19a/b-3p and FRK in the present study added to the complexity of this regulatory network. Furthermore, the pleiotropic nature of miRNAs dictates that miR-19 may be involved in more cellular processes in addition to cell proliferation. Additional studies are needed to identify target mRNAs regulated by miR-19, and thus elucidate the role of miR-19 in ccRCC. The diagnostic and prognostic values of miR-19 should also be explored in the future since the prognostic data from the TCGA KIRC indicate that high miR-19 expression is associated with poor survival for ccRCC patients. In addition, as ccRCC is resistant to conventional chemotherapy and radiotherapy, treatments targeting miR-19 can be considered in therapeutic strategies for ccRCC patients.

Conclusion

Collectively, our study identified FRK as a novel regulator of proliferation that was targeted by miR-19a-3p and miR-19b-3p. miR-19a/b-3p promotes the proliferation of ccRCC by targeting the FRK–PTEN axis (Figure 5H). These findings unravel a new mechanism involved in ccRCC proliferation regulation and may be useful in the identification of novel therapeutic targets for ccRCC.

Acknowledgments

This work was supported by National Natural Science Fund (Grant No 81672525), the Project of Liaoning Distinguished Professor (Grant No [2012]145), Liaoning Natural Science Fund (Grant No 201602830), Shenyang Plan Project of Science and Technology (Grant No F17-230-9-08), Shenyang Clinical Medicine Research Center (Grant No [2017]76), China Medical University's 2017 Discipline Promotion Program (Grant No 2017XK08), and China Medical University's 2018 Discipline Promotion Program.

Disclosure

The authors report no conflicts of interest in this work.

References

1. Ricketts CJ, Crooks DR, Sourbier C, Schmidt LS, Srinivasan R, Linehan WM. SnapShot: renal cell carcinoma. *Cancer Cell*. 2016; 29(4):610–610.e1. doi:10.1016/j.ccell.2016.03.021
2. Hsieh JJ, Purdue MP, Signoretti S, et al. Renal cell carcinoma. *Nat Rev Dis Primers*. 2017;3:17009. doi:10.1038/nrdp.2017.9
3. Lokeshwar SD, Talukder A, Yates TJ, et al. Molecular characterization of renal cell carcinoma: a potential three-microRNA prognostic signature. *Cancer Epidemiol Biomarkers Prev*. 2018;27(4):464–472. doi:10.1158/1055-9965.EPI-17-0700
4. Znaor A, Lortet-Tieulent J, Laversanne M, Jemal A, Bray F. International variations and trends in renal cell carcinoma incidence and mortality. *Eur Urol*. 2015;67(3):519–530. doi:10.1016/j.eururo.2014.10.002
5. He L, Hannon GJ. MicroRNAs: small RNAs with a big role in gene regulation. *Nat Rev Genet*. 2004;5(7):522–531. doi:10.1038/nrg1379
6. Croce CM. Causes and consequences of microRNA dysregulation in cancer. *Nat Rev Genet*. 2009;10(10):704–714. doi:10.1038/nrg2634
7. Gottardo F, Liu CG, Ferracin M, et al. Micro-RNA profiling in kidney and bladder cancers. *Urol Oncol*. 2007;25(5):387–392. doi:10.1016/j.urolonc.2007.01.019

8. White NMA, Bao TT, Grigull J, et al. miRNA profiling for clear cell renal cell carcinoma: biomarker discovery and identification of potential controls and consequences of miRNA dysregulation. *J Urol*. 2011; 186(3):1077–1083. doi:10.1016/j.juro.2011.04.110
9. Chow TF, Youssef YM, Lianidou E, et al. Differential expression profiling of microRNAs and their potential involvement in renal cell carcinoma pathogenesis. *Clin Biochem*. 2010;43(1–2):150–158. doi:10.1016/j.clinbiochem.2009.07.020
10. Grimson A, Farh KK-H, Johnston WK, Garrett-Engele P, Lim LP, Bartel DP. MicroRNA targeting specificity in mammals: determinants beyond seed pairing. *Mol Cell*. 2007;27(1):91–105. doi:10.1016/j.molcel.2007.06.017
11. Wang W, Zhang A, Hao Y, Wang G, Jia Z. The emerging role of miR-19 in glioma. *J Cell Mol Med*. 2018;22(10):4611–4616. doi:10.1111/jcmm.13788
12. Zhou J, Zhang X, Shi H, Fan C. MiR-19 regulates breast cancer cell aggressiveness by targeting profilin 1. *FEBS Lett*. 2017;591(11):1623. doi:10.1002/1873-3468.12657
13. Li Z, Cai J, Cao X. MiR-19 suppresses fibroblast-like synoviocytes cytokine release by targeting toll like receptor 2 in rheumatoid arthritis. *Am J Transl Res*. 2016;8(12):5512–5518.
14. Xiao W, Gao Z, Duan Y, Yuan W, Ke Y. Downregulation of miR-19a exhibits inhibitory effects on metastatic renal cell carcinoma by targeting PIK3CA and inactivating Notch signaling in vitro. *Oncol Rep*. 2015; 34(2):739–746. doi:10.3892/or.2015.4041
15. Niu S, Ma X, Zhang Y, et al. MicroRNA-19a and microRNA-19b promote the malignancy of clear cell renal cell carcinoma through targeting the tumor suppressor RhoB. *PLoS One*. 2018;13(2):e0192790. doi:10.1371/journal.pone.0192790
16. Cance WG, Craven RJ, Weiner TM, Liu ET. Novel protein kinases expressed in human breast cancer. *Int J Cancer*. 1993;54(4):571–577.
17. Craven RJ, Cance WG, Liu ET. The nuclear tyrosine kinase Rak associates with the retinoblastoma protein pRb. *Cancer Res*. 1995; 55(18):3969–3972.
18. Meyer T, Xu L, Chang J, Liu ET, Craven RJ, Cance WG. Breast cancer cell line proliferation blocked by the Src-related Rak tyrosine kinase. *Int J Cancer*. 2003;104(2):139–146. doi:10.1002/ijc.10925
19. Yim EK, Peng G, Dai H, et al. Rak functions as a tumor suppressor by regulating PTEN protein stability and function. *Cancer Cell*. 2009; 15(4):304–314. doi:10.1016/j.ccr.2009.02.012
20. Hua L, Zhu M, Song X, et al. FRK suppresses the proliferation of human glioma cells by inhibiting cyclin D1 nuclear accumulation. *J Neurooncol*. 2014;119(1):49–58. doi:10.1007/s11060-014-1461-y
21. Chen JS, Hung WS, Chan HH, Tsai SJ, Sun HS. In silico identification of oncogenic potential of fyn-related kinase in hepatocellular carcinoma. *Bioinformatics*. 2013;29(4):420–427. doi:10.1093/bioinformatics/bts715
22. Je DW, Ji YG, Cho Y, Lee DH. The inhibition of SRC family kinase suppresses pancreatic cancer cell proliferation, migration, and invasion. *Pancreas*. 2014;43(5):768–776. doi:10.1097/MPA.0000000000000103
23. Chandrashekar DS, Bashel B, Balasubramanya SAH, et al. UALCAN: a portal for facilitating tumor subgroup gene expression and survival analyses. *Neoplasia*. 2017;19(8):649–658. doi:10.1016/j.neo.2017.05.002
24. Ortega-Molina A, Serrano M. PTEN in cancer, metabolism, and aging. *Trends Endocrinol Metab*. 2013;24(4):184–189. doi:10.1016/j.tem.2012.11.002
25. Song MS, Salmena L, Pandolfi PP. The functions and regulation of the PTEN tumour suppressor. *Nat Rev Mol Cell Biol*. 2012;13(5):283–296. doi:10.1038/nrm3330
26. Yang JH, Li JH, Shao P, Zhou H, Chen YQ, Qu LH. starBase: a database for exploring microRNA-mRNA interaction maps from Argonaute CLIP-Seq and Degradome-Seq data. *Nucleic Acids Res*. 2011; 39(Database issue):D202–D209. doi:10.1093/nar/gkq1056
27. Li JH, Liu S, Zhou H, Qu LH, Yang JH. StarBase v2.0: decoding miRNA-ceRNA, miRNA-ncRNA and protein-RNA interaction networks from large-scale CLIP-Seq data. *Nucleic Acids Res*. 2014; 42(Database issue):D92–D97. doi:10.1093/nar/gkt1248
28. Hosoya N, Qiao Y, Hangaishi A, et al. Identification of a SRC-like tyrosine kinase gene, FRK, fused with ETV6 in a patient with acute myelogenous leukemia carrying a t(6;12)(q21;p13) translocation. *Genes Chromosomes Cancer*. 2005;42(3):269–279. doi:10.1002/gcc.20147
29. Zhang J, Shen Z, Liu H, Liu S, Shu W. Diagnostic potential of methylated DAPK in brushing samples of nasopharyngeal carcinoma. *Cancer Manag Res*. 2018;10:2953–2964. doi:10.2147/CMAR.S171796
30. Chow TF, Mankaruos M, Scorilas A, et al. The miR-17-92 cluster is over expressed in and has an oncogenic effect on renal cell carcinoma. *J Urol*. 2010;183(2):743–751. doi:10.1016/j.juro.2009.09.086
31. Liang Z, Li Y, Huang K, Wagar N, Shim H. Regulation of miR-19 to breast cancer chemoresistance through targeting PTEN. *Pharm Res*. 2011;28(12):3091–3100. doi:10.1007/s11095-011-0570-y
32. Li X, Xie W, Xie C, et al. Curcumin modulates miR-19/PTEN/AKT/p53 axis to suppress bisphenol A-induced MCF-7 breast cancer cell proliferation. *Phytother Res*. 2014;28(10):1553–1560. doi:10.1002/ptr.5167

Supplementary materials

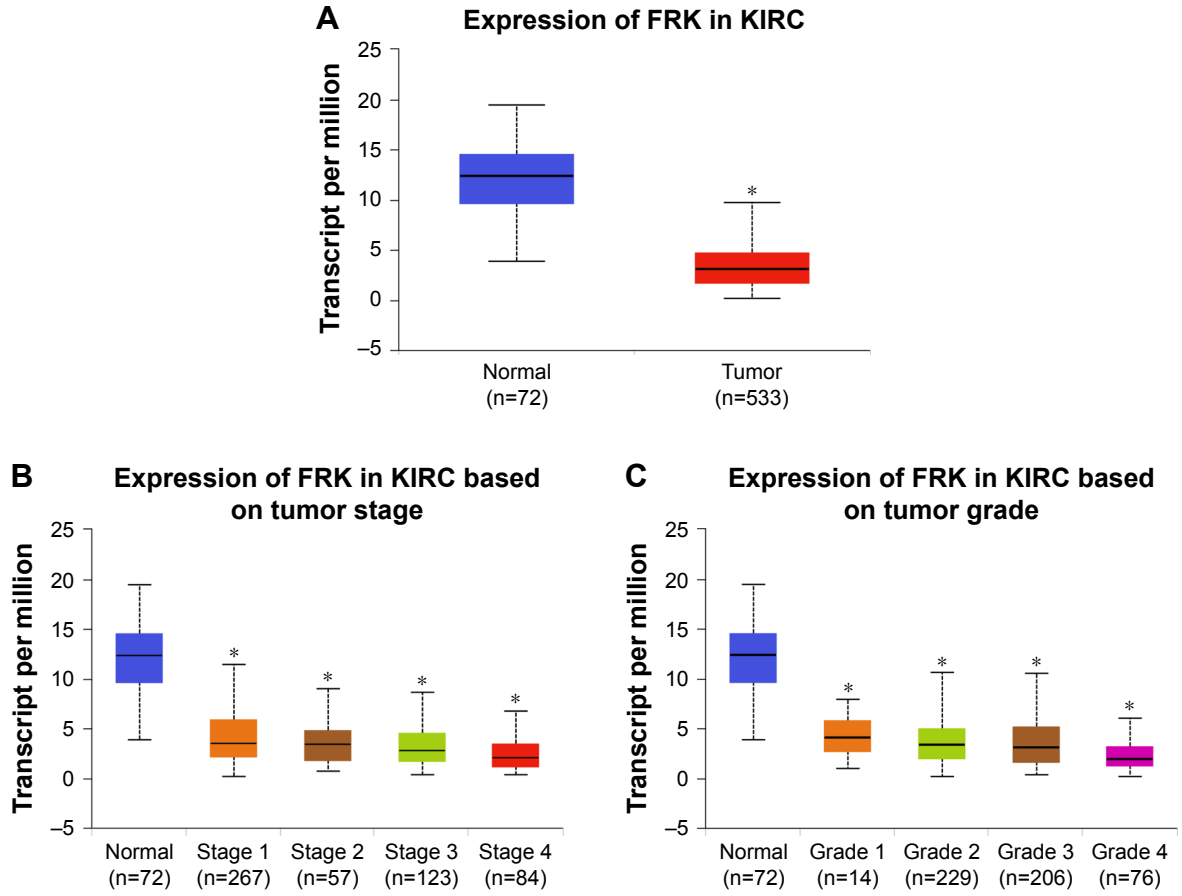

Figure S1 (**A**) FRK transcript levels in ccRCC tissues and normal renal tissues based on KIRC data set from TCGA. (**B**, **C**) FRK transcript levels in ccRCC of different stages and grades based on KIRC data set from TCGA (*$P<0.05$).
Abbreviation: ccRCC, clear cell renal cell carcinoma.

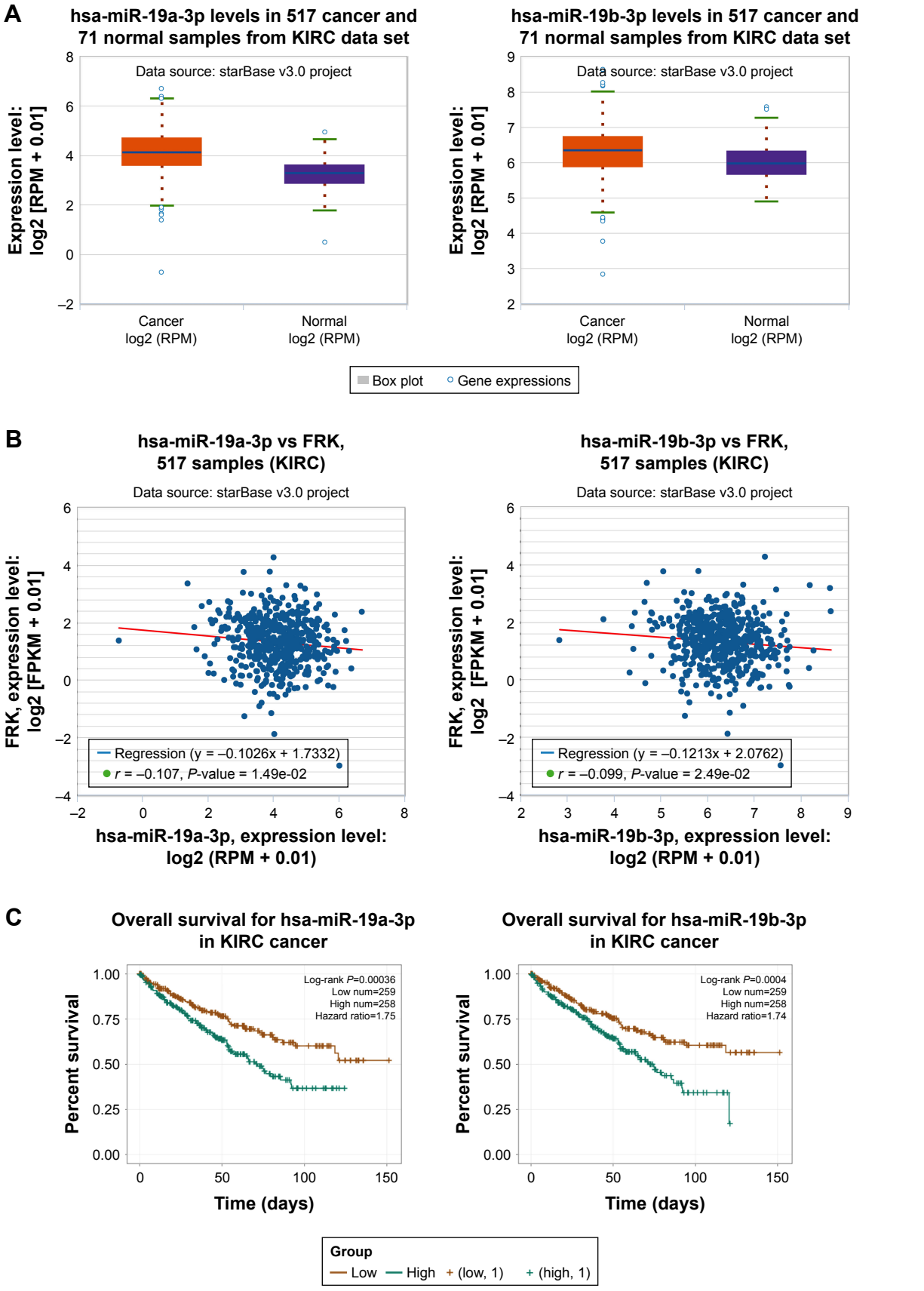

Figure S2 (**A**) Expression of miR-19a-3p and miR-19b-3p based on TCGA KIRC data set. (**B**) The expression level of miR-19a/b-3p was negatively correlated with the expression level of FRK from TCGA KIRC data set. (**C**) Kaplan–Meier curve for overall survival of patients with high (n=258) and low (n=259) miR-19a/b-3p expression level based on TCGA KIRC data set.

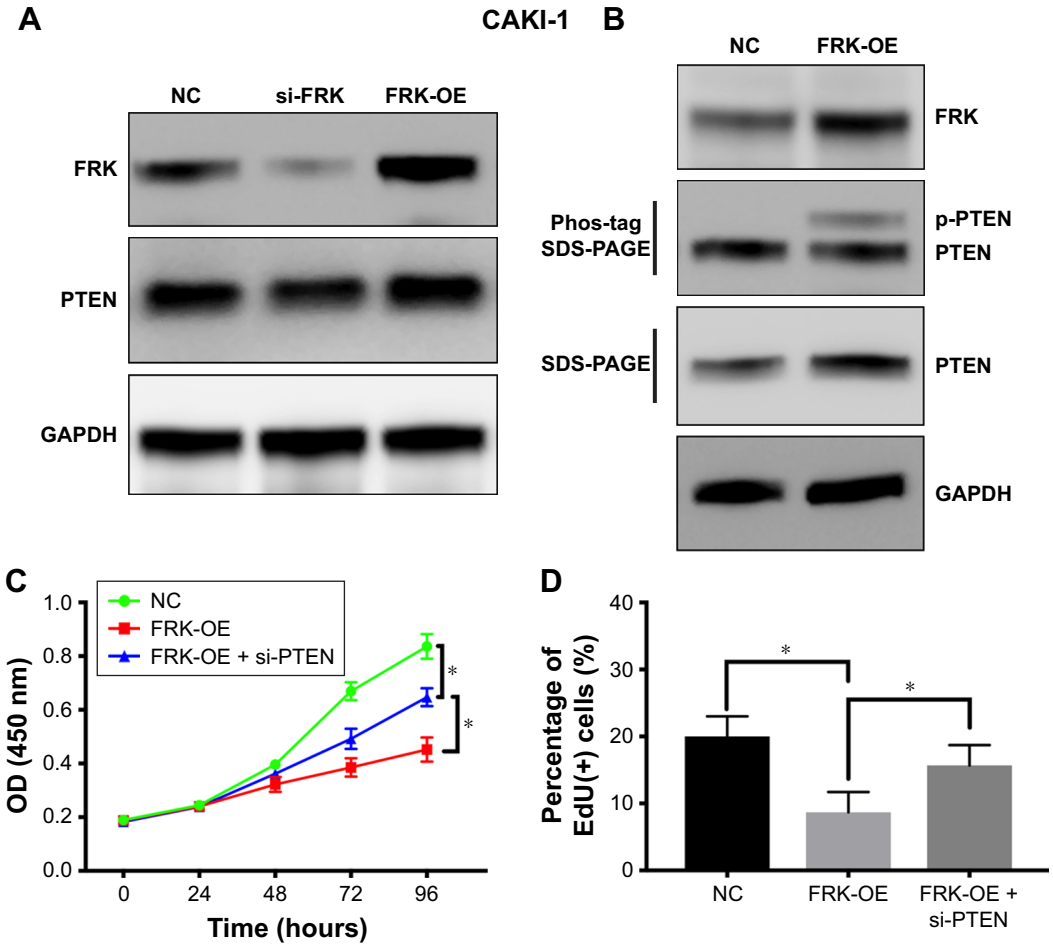

Figure S3 (**A**) Immunoblot analysis of PTEN in CAKI-1 cells following FRK knockdown or overexpression. (**B**) The effects of FRK overexpression on the phosphorylation of PTEN in CAKI-1 cells were analyzed by a Phos-tag assay. Immunoblots for total PTEN were also performed on normal SDS-PAGE gels. (**C**, **D**) The effects of FRK overexpression with or without si-PTEN on the proliferation of ACHN cells were analyzed by CCK-8 and EdU incorporation assays. *$P<0.05$.
Abbreviation: EdU, 5-ethynyl-2′-deoxyuridine.

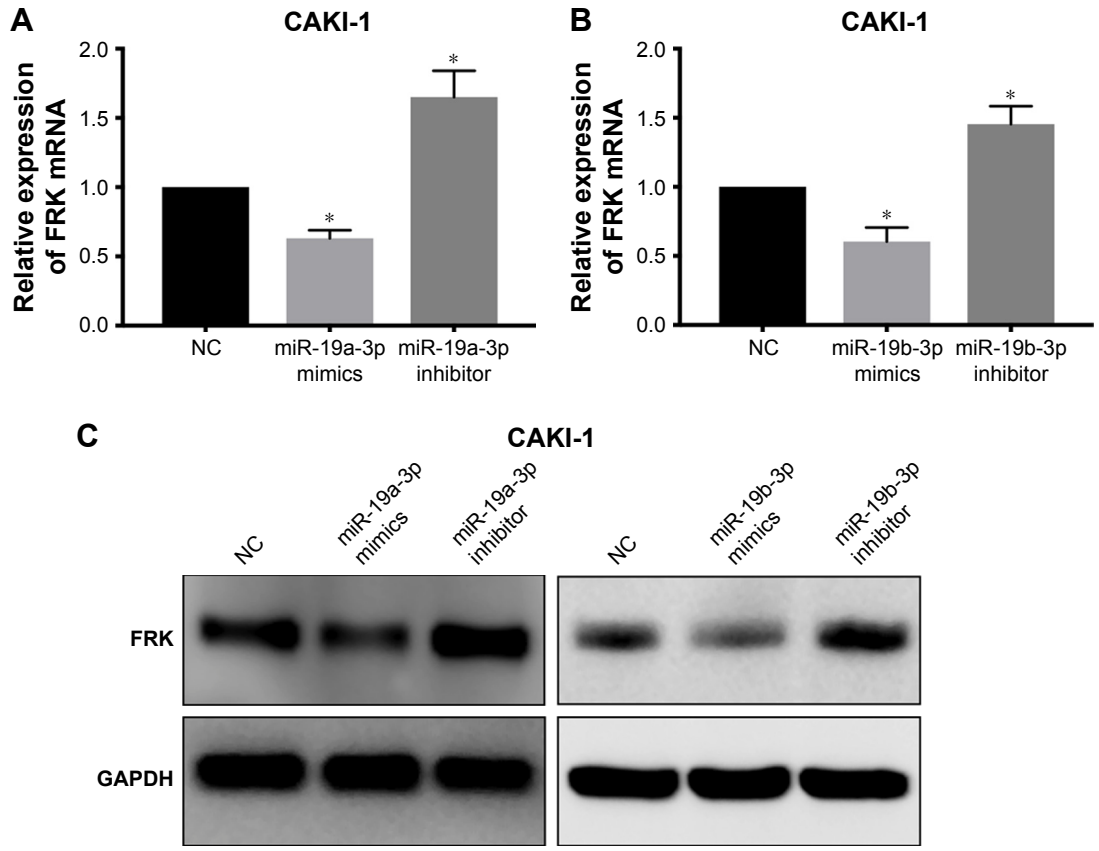

Figure S4 (**A**, **B**) The mRNA expression of FRK in CAKI-1 cells after transfecting with miR-19a/b-3p mimics or inhibitors is presented as bar graphs. (**C**) The protein expression of FRK in CAKI-1 cells after transfecting with miR-19a/b-3p mimics or inhibitors was analyzed by immunoblotting. *$P<0.05$.